Supporting Information

Synergistic bimetallic PdAg nanoalloy for electrocatalytic reduction of nitrate to ammonia in neutral solution

Yu-Chi Tseng, Zih-Syun Lin, Chih-Ting Lu, Min-Chieh Chuang, Cheng-Che Tsai, Tzung-Wen Chiou*

Department of Chemistry, Tunghai University, Taichung 407224, Taiwan

Email: twchiou@thu.edu.tw (TWC)

Experimental section

Chemicals. $Pd(NO_3)_2$ (99.8 %), $NaNO_2$ (98 %), potassium citrate tribasic monohydrate (99.0 %), NH_4Cl (99.5 %), sodium hypochlorite solution (11-15 %) were purchased from Thermo scientific. $AgNO_3$ (99.0 %) was bought from Fluorochem. K_2SO_4 (99.0 %) and KOH (85 %) were purchased from Duksan. Salicylic acid (98 %), sodium nitroferricyanide dihydrate (99.5 %), p-aminobenzenesulfonamide (99.6 %) and 5,5-Dimethyl-1-pyrroline N-Oxide (DMPO, 99.8 %) were purchased from BLD Pharmatech Ltd. KNO_3 (99 %) and H_3PO_4 (85 %) were bought from Honeywell. H_2SO_4 was bought from Union Chemical Works LTD (Taiwan). N-(1-Naphthyl)ethylenediamine dihydrochloride (98 %), deuterium oxide (99.9 %)and potassium nitrate-^{15}N (99 %) were purchased from Merek. All chemicals were used directly without further purification. Ultrapure water (18.2 MΩ) used in the experiments was supplied by a Millipore System (Direct-Q® 3).

Preparation of Catalysts. The electrodeposition was carried out with a standard three-electrode electrochemical cell containing nickel foam (surface area: 0.25 cm^2), a graphite rod (L 100 mm, diam. 3 mm) and a saturated calomel electrode (SCE) as the working, auxiliary and reference electrodes, respectively. In order to the many physical characterizations, electrodepositions on graphite plate electrodes as the working electrode were performed. The electrolyte solution of PdAg alloy was prepared; $Pd(NO_3)_2$ (0.0161 g, 0.07 mmol), $AgNO_3$ (0.0595 g, 0.35 mmol) and potassium citrate tribasic monohydrate (5.6771 g, 0.0175 mol) were dissolved in 35 mL DI water. The electrolyte solution of Pd NP was prepared; $Pd(NO_3)_2$ (0.0161 g, 0.07 mmol) and potassium citrate tribasic monohydrate (5.6771 g, 0.0175 mol) were dissolved in 35 mL DI water. The electrolyte solution of Ag NP was prepared; $AgNO_3$ (0.0595 g, 0.35

mmol) and potassium citrate tribasic monohydrate (5.6771 g, 0.0175 mol) were dissolved in 35 mL DI water. All materials were prepared though controlled potential electrolysis at −1.644 V (vs SCE) for 500 s at ambient temperature. After deposition, the materials by careful rinse with water were directly used for electrochemistry tests.

Physical characterization. Powder X-ray diffraction (pXRD) data were obtained using a Rigaku MiniFlex X-ray Powder Diffractometer with a Cu K-α radiation source in the range 2θ = 5-100°. Scanning electron microscopy (SEM) images were obtained with a JSM-6510 microscope (JEOL) equipped. The morphologies of samples were characterized on a transmission electron microscope (TEM, JEOL JEM-1400, Japan) by dropping sample solutions on Cu grids. HRTEM images were obtained with a JEM-2010 microscope (JEOL) equipped. X-ray photoelectron spectroscopy (XPS) spectra were collected on a ULVAC-PHI XPS spectrometer equipped with a monochromatized 1486.6 eV Al Kα X-ray line source directed 45° with respect to the sample surface. The spectra were registered at a base pressure of $<5\times10^{-10}$ torr. Low-resolution survey scans were acquired with a 100 μm spot size between the binding energies of 1-1100 eV. High-resolution scans with a resolution of 0.2 eV were collected between 330-355 (for Pd) and 362-382 (for Ag) eV. The electron paramagnanetic resonance (EPR) measurements of DMPO were carried out at a Bruker EMX-plus using an ER 4122 SHQE resonator.

Electrochemical measurements. All electrochemical experiments were performed with a CH Instrument 405 potentiostat. Fundamental electrochemical testing was carried out, consisting of samples as the working electrode, a graphite rod (L 100 mm, diam. 3 mm) auxiliary electrode and a saturated calomel electrode (SCE) reference electrode in H-type cell. The H-type cell was separated by Nafion 117 membrane. All

potentials reported in this paper were converted from vs SCE to vs reversible hydrogen electrode (RHE). RHE = SCE + 0.244 + 0.059×pH. Note that the change in pH of the electrolyte during the reaction is negligible. In all experiments, the iR compensation was performed by CHI model 405 software. The linear sweep voltammetry (LSV) curves were obtained in 0.5 M K_2SO_4 solution with/without 0.1 M KNO_3 at a scan rate of 2 mV/s. Tafel slopes were calculated using the Polarization curves by plotting overpotential against log(current density). Controlled potential electrolysis (CPE) experiments were conducted in 0.5 M K_2SO_4 solution with 0.1 M KNO_3 stirred constantly. The electrochemically active surface area (ECSA) was evaluated in terms of double-layer capacitance (C_{DL}). Cyclic voltammogram (CV) scans were conducted in static solution by sweeping the potential from the more positive to negative potential and back at 5 different scan rates: 20, 40, 60, 80 and 100 mV s^{-1}. The capacitance was determined from the tenth CV curve of each scan rate. The electrochemical double-layer capacitance, C_{DL}, as given by $i_c = vC_{DL}$ (i_c: current density from CV, v: scan rate). We used the specific capacitance (C_S) of 0.040 mF cm^{-2} (0.196 cm^2) in the following calculations of the ECSA.[1] The ECSA of the catalysts can be calculated by dividing C_{DL} by C_S, ECSA = C_{DL}/C_s. The electrochemical impedance spectroscopy (EIS) measurements were carried out in a frequency range of 0.1 Hz to 100 kHz with an amplitude of 5 mV at −0.04 V (vs RHE). The curve fitting was performed by Zview software.

ICP-MS experiment. ICP-MS was performed on a Thermo Scientific™ Element 2™ (Germany). Dry sample was dissolved in concentrated HNO_3.

Determination of NH_3. The concentration of NH_3 was spectrophotometrically determined by the indophenol blue method. The 2 mL of post-NO_3RR electrolyte was

collected from the electrochemical reaction vessel. Then 2 mL of a 1 M KOH solution containing 5 wt % salicylic acid and 5 wt% potassium citrate tribasic monohydrate was added, followed by the addition of 1 mL of 0.05 M NaClO and 0.2 mL of 1 wt % sodium nitroferricyanide aqueous solution. After the chromogenic reaction for 2 h at room temperature, the absorption spectrum was measured using an UV–vis spectrophotometer (BMG SPECTROstar^{Nano}). The absorbance at 655 nm was used to determine the concentration of NH_3. The calibration curve was obtained by using a series of standard NH_4Cl solutions in the same operation.

Determination of NO_2^-. The concentration of NO_2^- was spectrophotometrically determined by the Griess test. The Griess agent was prepared by dissolving N-(1-naphthyl)ethyldiamine dihydrochloride (800 mg), sulfonamide (40 mg) and H_3PO_4 (2 mL, 85%) into 10 ml of DI water. The 2 mL of post-NO_3RR electrolyte was collected from the electrochemical reaction vessel, and then the solutions (2 mL) were mixed with the Griess agent (40 μL). After the chromogenic reaction for 10 min at room temperature, the absorption spectrum was measured using an UV–vis spectrophotometer. The absorbance at 540 nm was used to determine the concentration of NO_2^-. The calibration curve was obtained by using a series of standard $NaNO_2$ solutions in the same operation.

Determinations of H_2. Quantification of the produced H_2 gas was performed by gas chromatography (Chromatec-Crystal 9000) equipped with a micropacked column (ShinCarbon ST #19808, Restek) and thermal conductivity detector (TCD). Helium was used as the carrier gas. Calibration curves were built by the injection of the known amounts of pure H_2. The amounts of H_2 dissolved in the solution were corrected by the Henry's law (K_H = 7.8 × 10-4 mol/atm·L for H_2).

Faradaic efficiency (FE %) = (V_{H2}/24.5)×100%/(Q_{CPE}/2F)

where V_{H2} is the volume (L) of H_2 gas by GC detection, Q_{CPE} is the charge (C) during CPE and F is the Faraday constant.

Determination of N_2H_4. The concentration of N_2H_4 was spectrophotometrically determined by the Watt and Chrisp test. The Watt and Chrisp agent was prepared by mixing hydrochloric acid (HCl, conc., 10.0 mL), ethanol (100 mL), and p-dimethylaminobenzaldehyde (2.00 g). The 1.50 mL of post-NO_3RR electrolyte was collected from the electrochemical reaction vessel, and then the solutions were mixed with the Watt and Chrisp agent (1.50 mL). After the chromogenic reaction for 30 min at room temperature in the dark, the absorption spectrum was measured using an UV–vis spectrophotometer. The absorbance at 460 nm was used to determine the concentration of N_2H_4. The calibration curve was obtained by using a series of standard N_2H_4 solutions in the same operation.

Determination of NH_3 by the ^{1}H NMR spectroscopy. The ^{1}H NMR spectroscopy was collected on a BRUKER Ascend TM 400MHz NMR spectrometer. The 0.5 mL of post-NO_3RR electrolyte was collected from the electrochemical reaction vessel, and then the solutions were mixed with maleic acid (MA, as the internal standard) aqueous solution (80 μL, 10 mM), H_2SO_4 solution (10 μL, 4 M) and DMSO-d_6 (10 μL). Next, 0.6 ml of the sample solution was sealed into an NMR tube (5 mm in diameter, 400 MHz). The quantitation of NH_3 can be determined by calculating the integral areas (*I*) of the peaks for MA (6.25 ppm, 2H) and for NH_4^+ (7.18 ppm, 4H) based on the followed equation:

$$C_{NH4+} = \frac{I_{NH4+}/4}{I_{MA}/2} \times C_{MA}$$

where C_{NH4+} and C_{MA} are the concentrations of NH_4^+ and MA in NMR tubes, and I_{NH4+}

and I_{MA} are the integral areas of the peaks for NH_4^+ and MA. The ^{15}N isotopic labeling experiment was conducted in a 0.5 M K_2SO_4 solution with 0.1 M $Na^{15}NO_3$ for the same operation described above.

EPR experiment. Radical capture experiments were performed in electrolytes with/without NO_3^-. After 2000 s of NO_3RR reaction at the potential of –0.44 V, 3.0 mL of the electrolyte was collected from the electrochemical reaction vessel and mixed with 30 mg of DMPO. Then the mixture was transferred to an EPR tube for detection.

Calculation of NH_3 FE, NO_2^- FE, N_2H_4 FE and NH_3 yield rate. The NH_3 FE was calculated as follows:

$$FE_{NH3} = \frac{8F \times C_{NH3} \times V}{Q}$$

where F is the Faraday constant (96485 C/mol), C_{NH3} is the detected concentration of NH_3 (M), V is the volume of the electrolyte, and Q is the total charge passed through the working electrode (C).

The NO_2^- FE was calculated as follows:

$$FE_{NO2-} = \frac{2F \times C_{NO2-} \times V}{Q}$$

where C_{NO2-} is the detected concentration of NO_2^- (M).

The N_2H_4 FE was calculated as follows:

$$FE_{N2H4} = \frac{7F \times C_{N2H4} \times V}{Q}$$

where C_{N2H4} is the detected concentration of N_2H_4 (M).

The NH_3 yield rate (YR) was calculated as follows:

$$YR_{NH3} = \frac{C_{NH3} \times V}{m \times t}$$

where m is the mass of electrocatalyst and t is time during the NO_3RR.

CO adsorption experiments: CO adsorption was conducted in 0.5 M K_2SO_4 and 0.1 M KNO_3 solution with CO bubbling for 20 min. Then, the electrolyte was saturated with argon by bubbling argon for 20 min. During all the above processes, LSV scans were conducted.

in situ **infrared reflection absorption spectroscopy experiments**. *In situ* infrared reflection absorption spectra was measured on a Bruker INVENIO R FT-IR spectrometer equipped with an MCT detector and cooled by liquid nitrogen during the electrochemical process. The NO_3RR was performed in the VeeMAX III (PIKE Technologies) accessory with three-electrode, in which the SCE and Pt plate were used for the reference and counter electrode, respectively. The working electrode was prepared as followed: A ~25-nm-thick ITO film was pre-deposited on the internal reflection element (IRE) of a 60° Si face angled crystal assembled with the J1 Jackfish spectroelectrochemical cell, after which the catalyst PdAg alloy was electrodeposited on the ITO film. *In situ* infrared reflection absorption spectra were recorded in electrolyte with NO_3^- by the potential from +0.757 V to −0.643 V vs. RHE. The spectrum collected at OCP was used for background subtraction.

Reference

1. C. C. L. McCrory, S. Jung, J. C. Peters, T. F. Jaramillo, *J. Am. Chem. Soc.*, 2013, **135**, 16977−16987.

a.

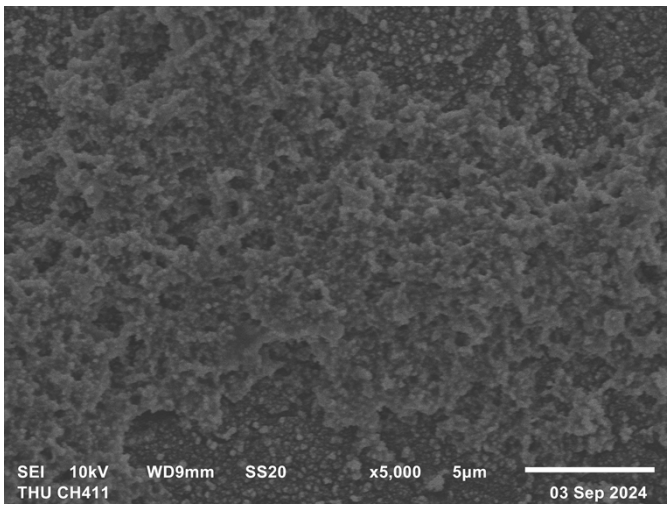

b.

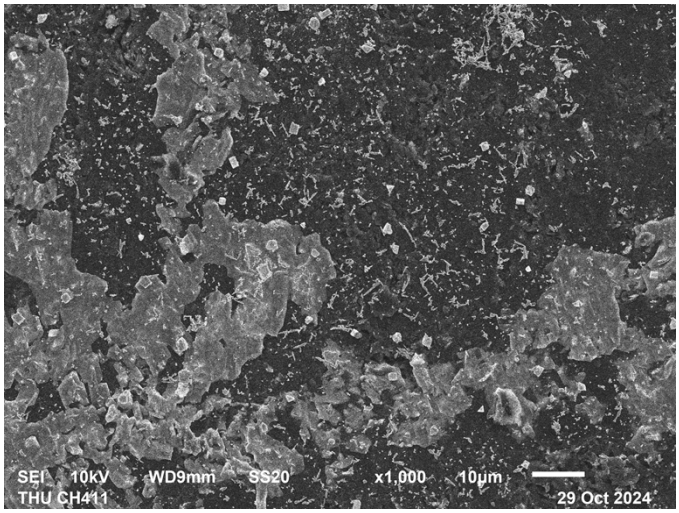

Figure S1. SEM images of (a) Pd NP and (b) Ag NP.

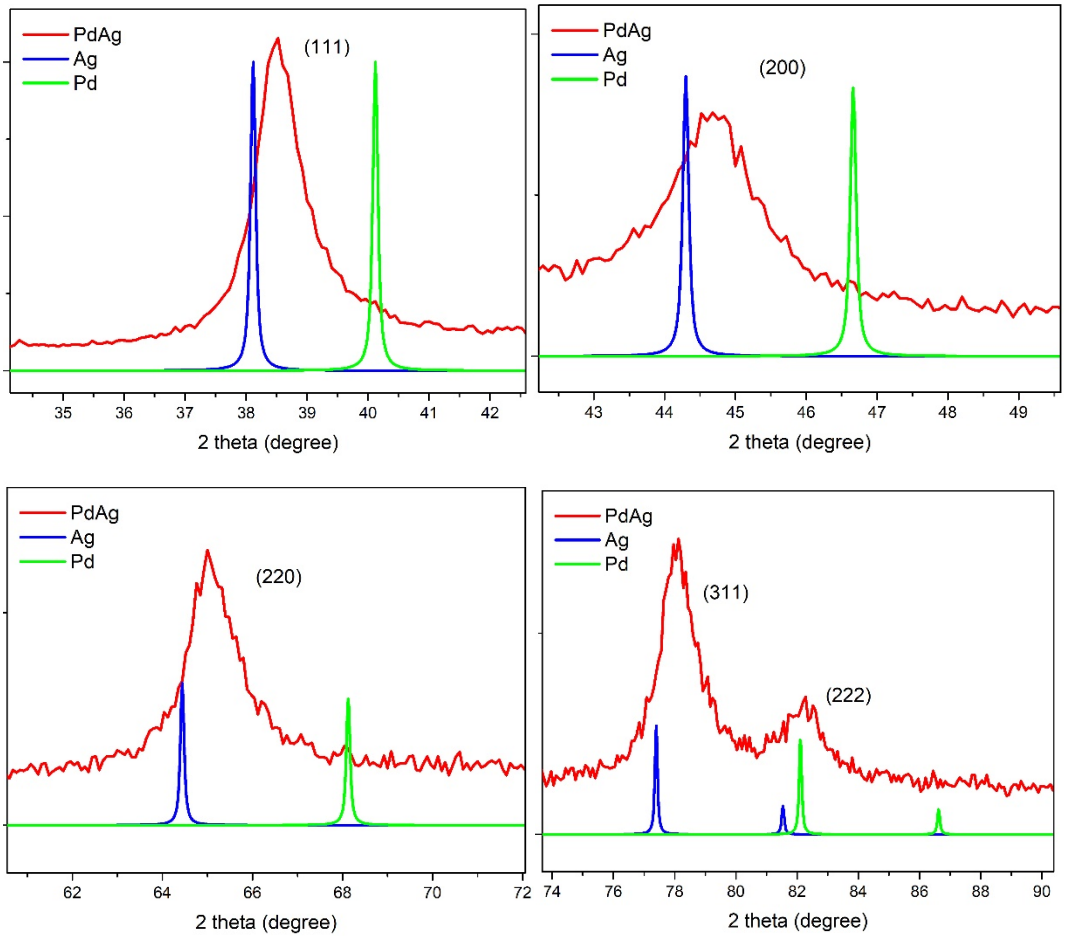

Figure S2. XRD patterns of PdAg alloy, metallic Ag and Pd.

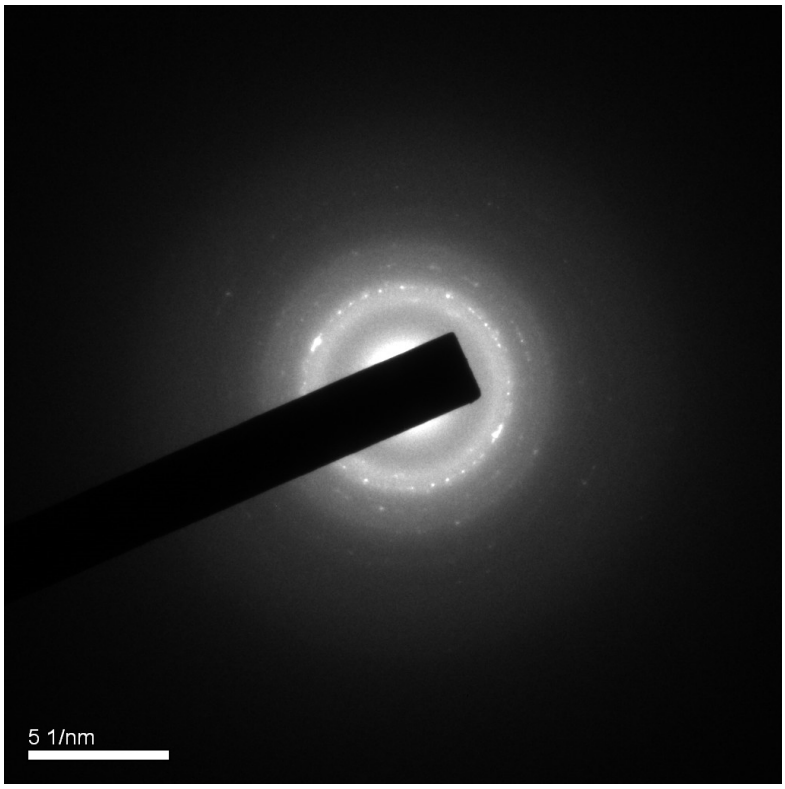

Figure S3. Selected-area electron diffraction pattern of PdAg alloy.

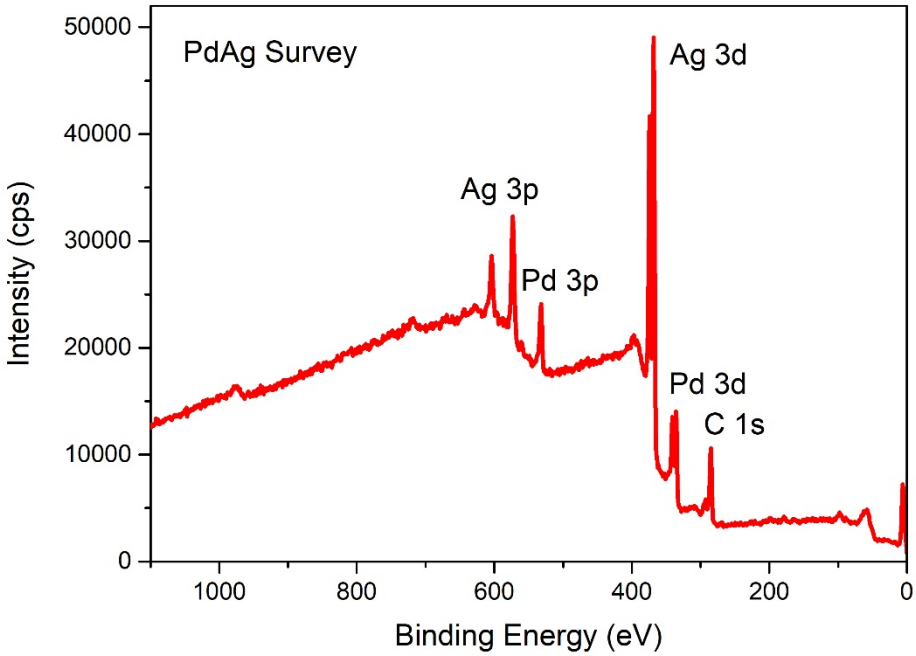

Figure S4. The survey XPS spectrum of PdAg alloy.

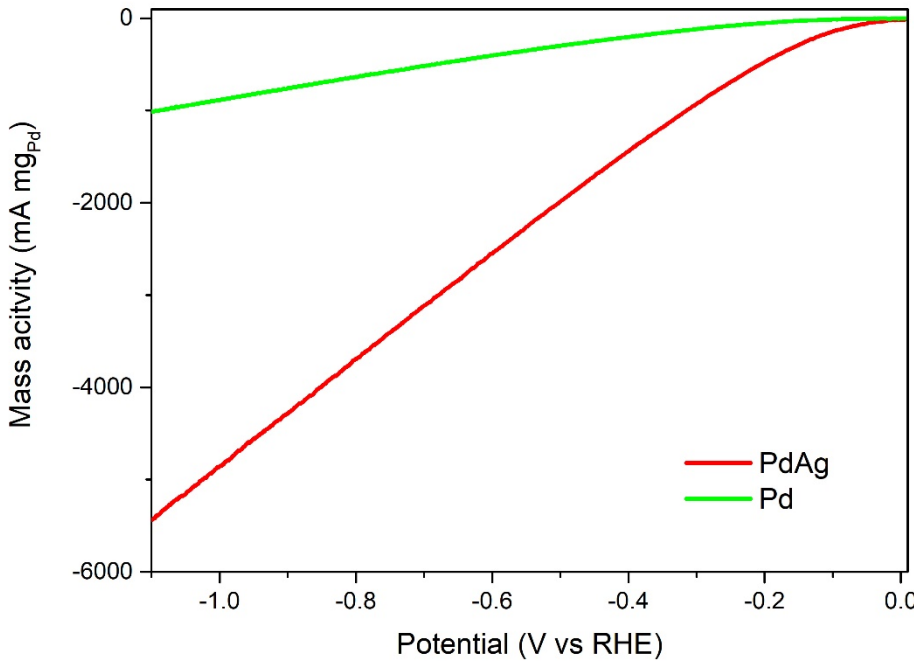

Figure S5. Mass activity of PdAg alloy and Pd NP.

a.

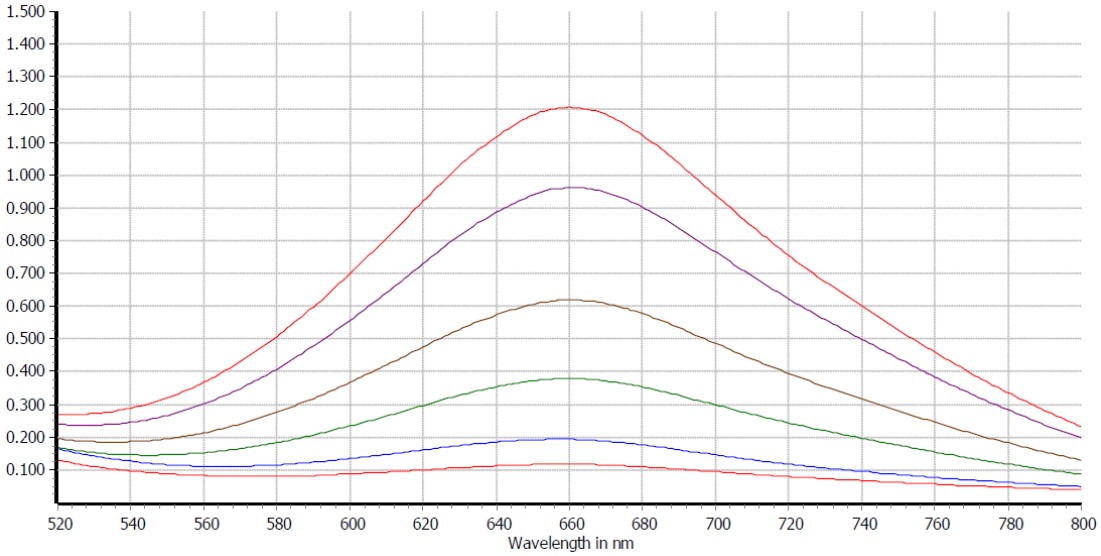

b.

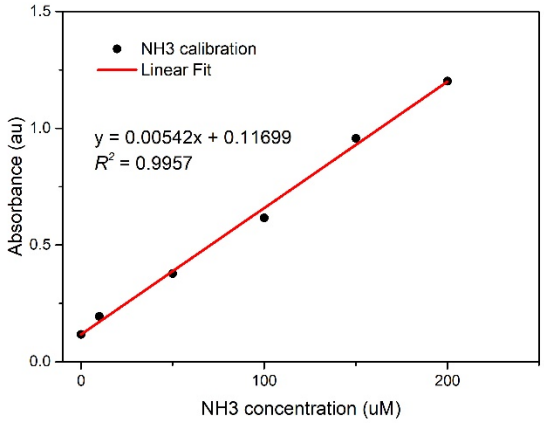

Figure S6. The indophenol blue spectrophotometric method. (a) UV-Vis spectra of solutions with different ammonia concentrations. (b) The linear standard curve for the calculation of ammonia production.

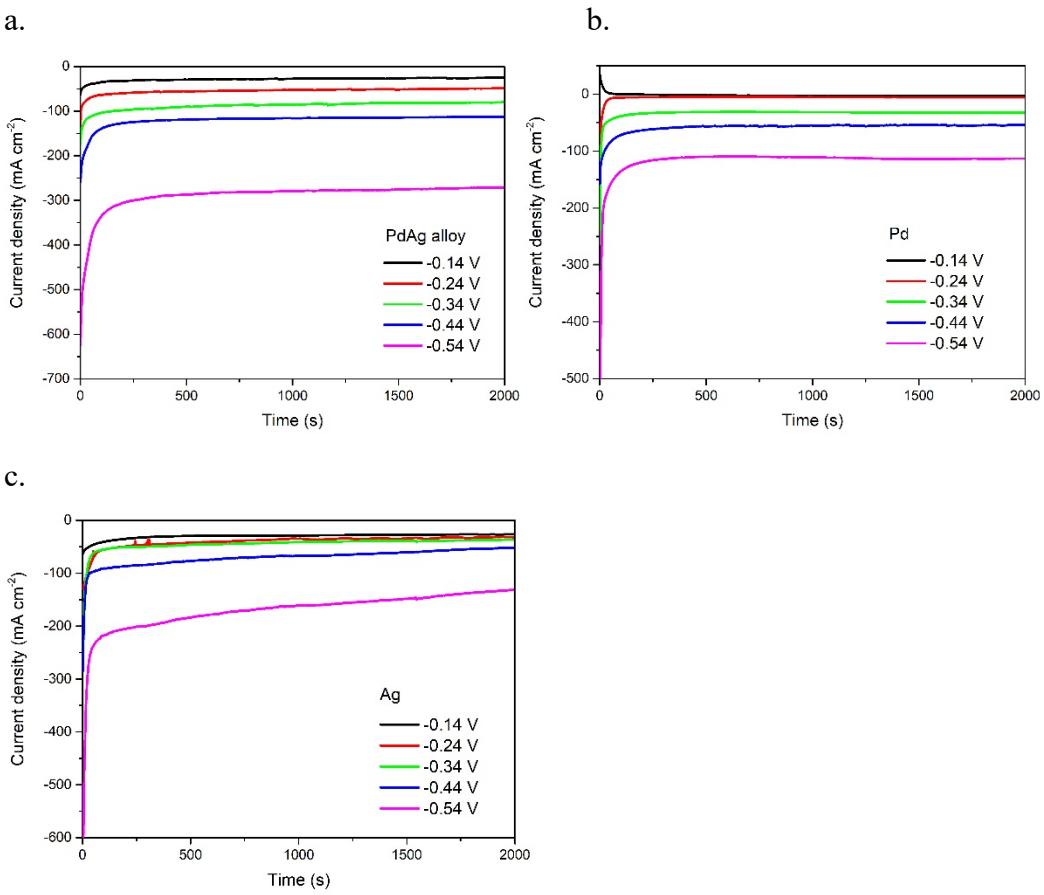

Figure S7. CPE current densities of (a) PdAg alloy, (b) Pd NP and (c) Ag NP at different potentials.

a.

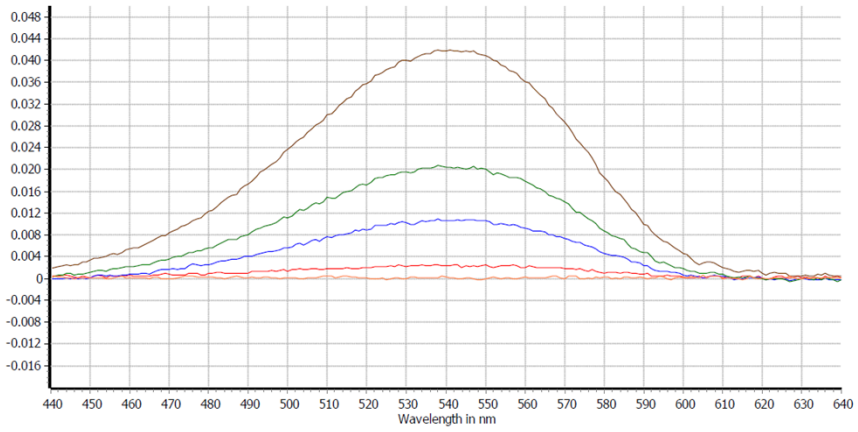

b.

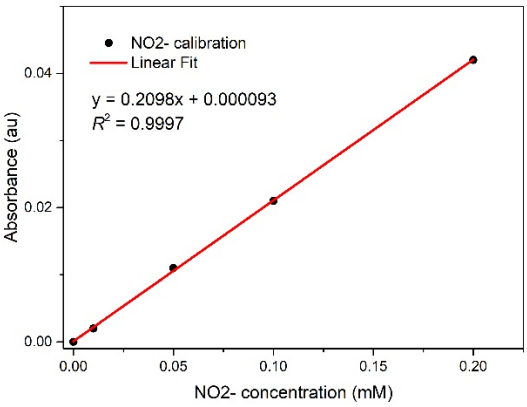

Figure S8. The colorimetric Griess test. (a) UV-Vis spectra of solutions with different NO_2^- concentrations. (b) The linear standard curve for the calculation of NO_2^- production.

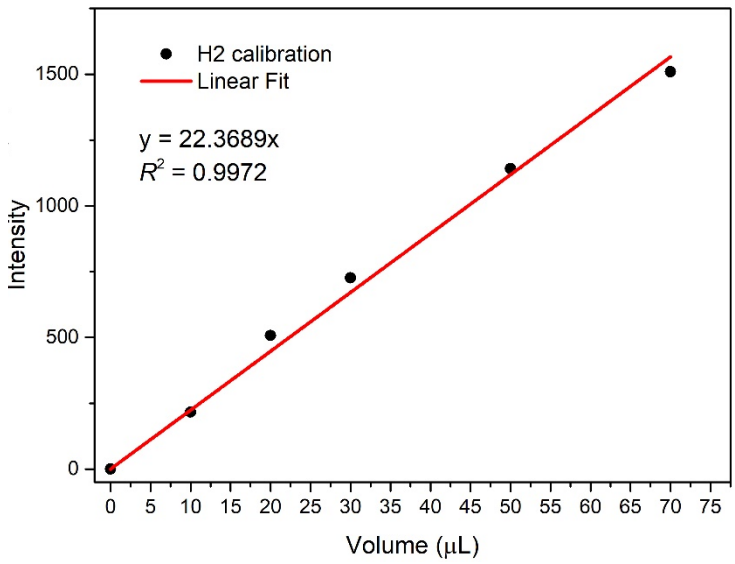

Figure S9. The linear standard curve for the calculation of H_2 production.

a.

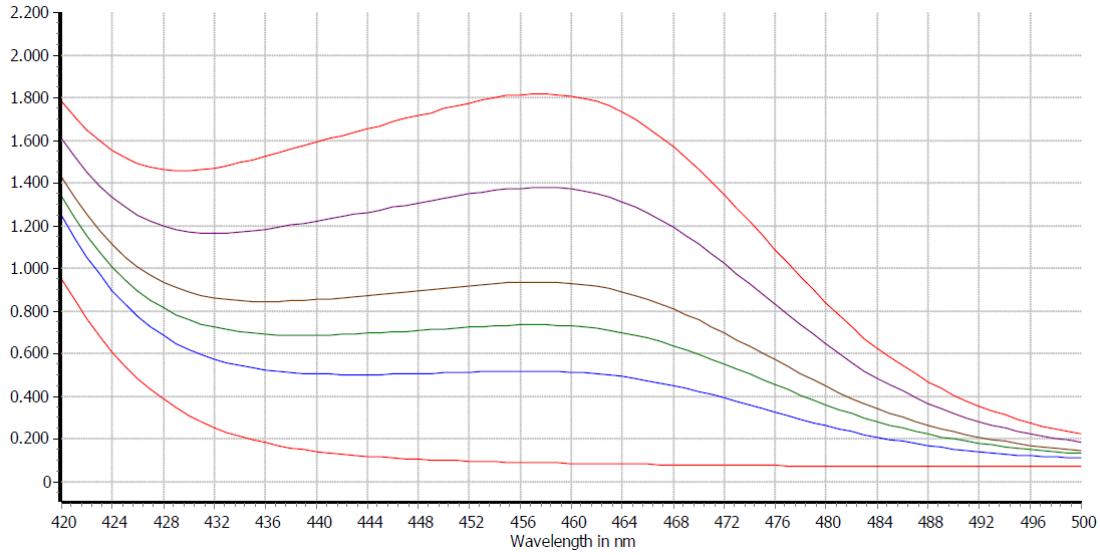

b.

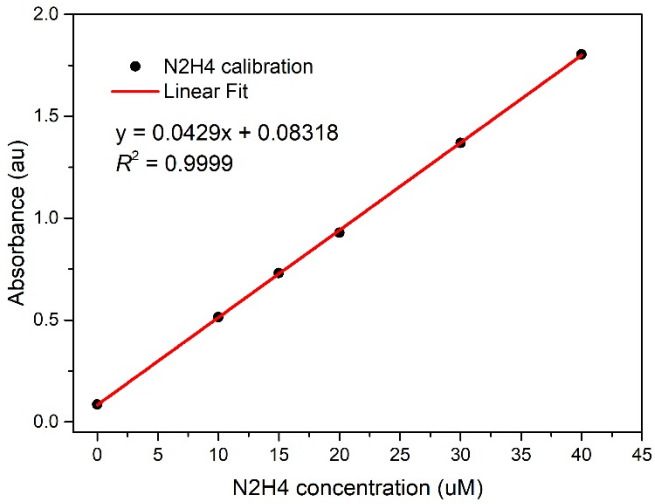

Figure S10. The colorimetric Watt and Chrisp test. (a) UV-Vis spectra of solutions with different N_2H_4 concentrations. (b) The linear standard curve for the calculation of N_2H_4 production.

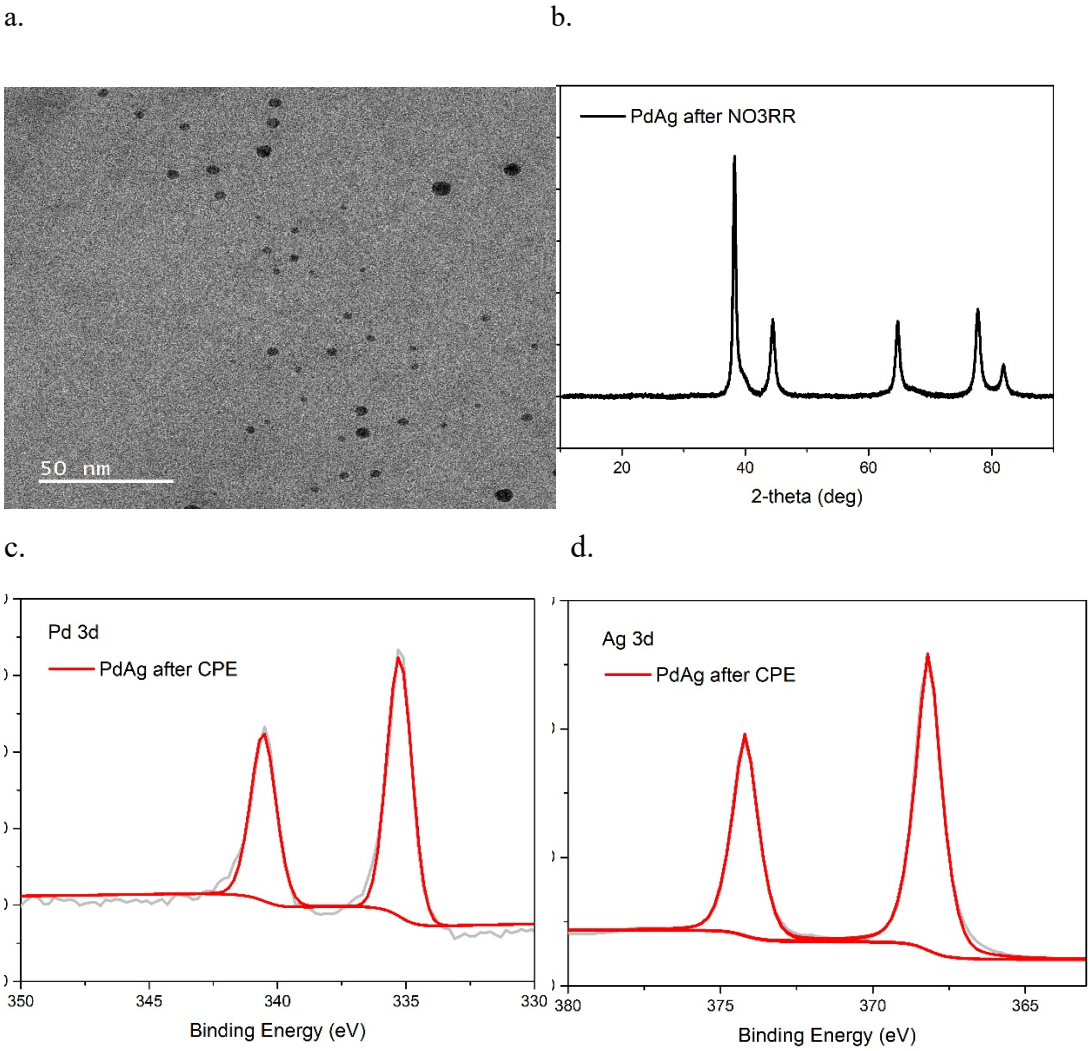

Figure S11. The (a) TEM image, (b) XRD patterns, (c) Pd 3d and (d) Ag 3d XPS spectra of PdAg alloy after NO_3RR.

a.

b.

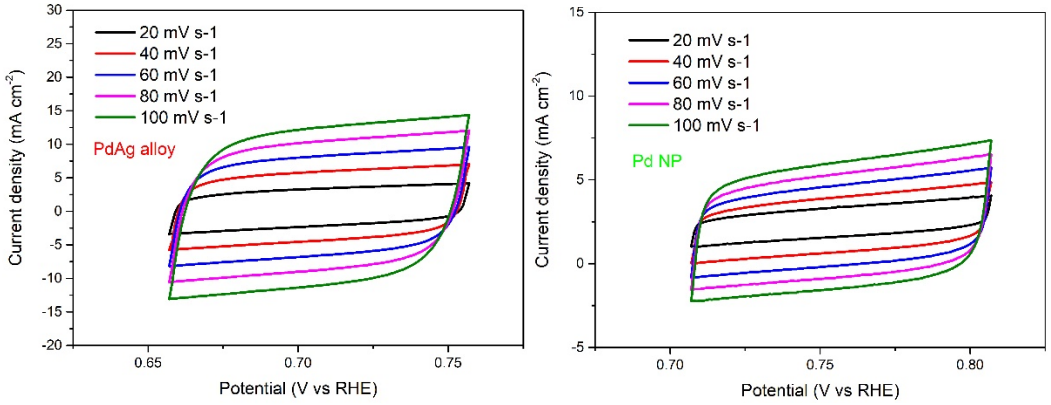

c.

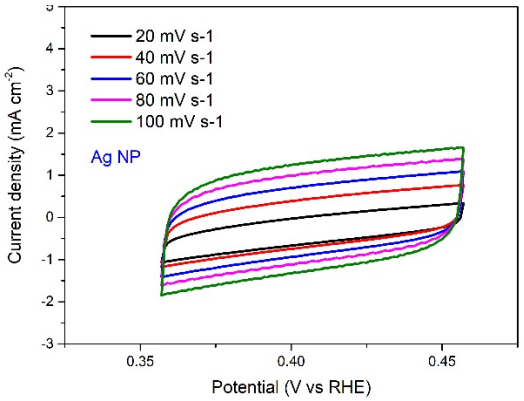

Figure S12. CV curves of (a) PdAg alloy, (b) Pd NP and (c) Ag NP at different scan rates.

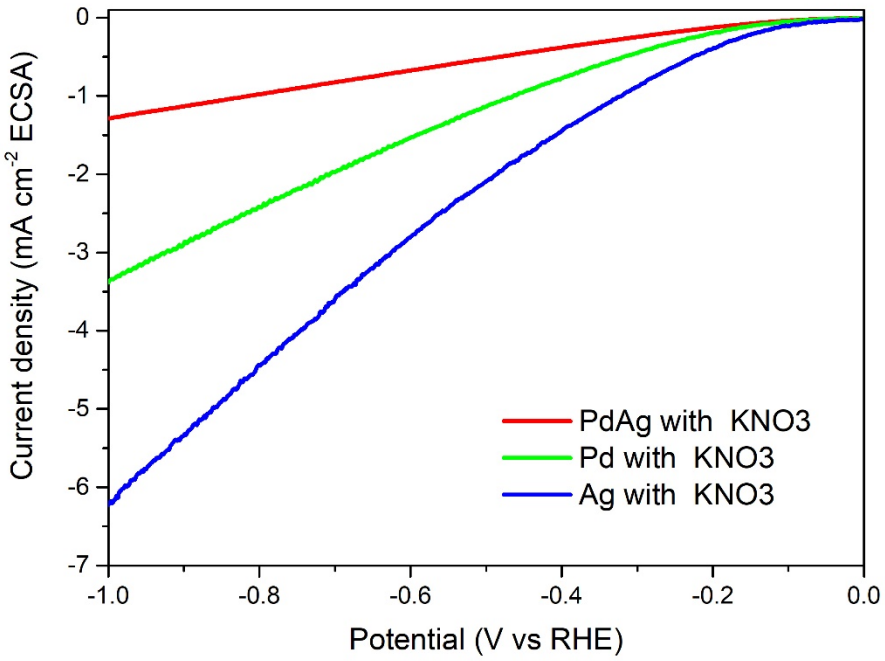

Figure S13. LSV curves normalized by the electrochemical active surface area (ECSA).

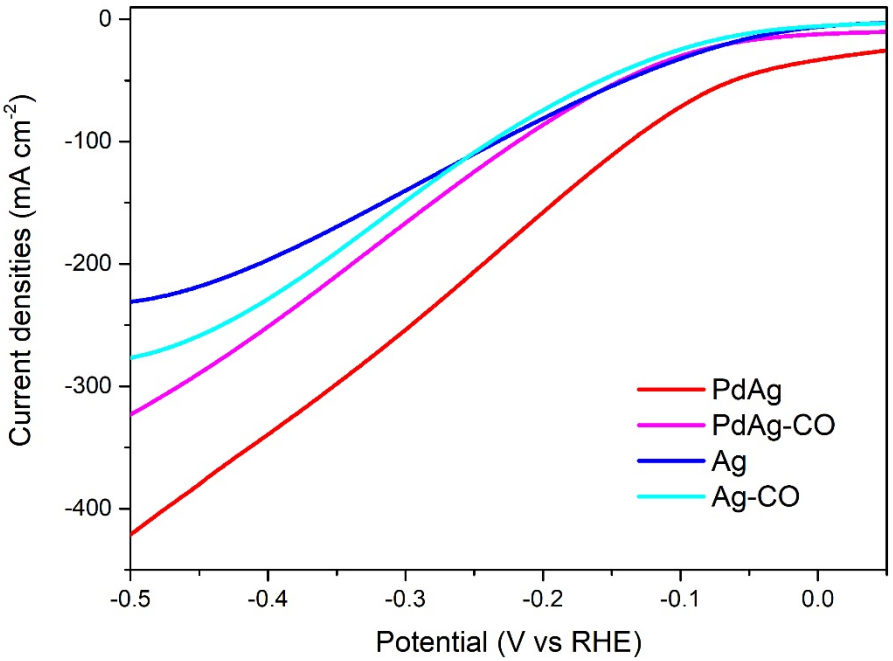

Figure S14. LSV curves of PdAg alloy and Ag NP without/with CO adsorption in 0.5 M K_2SO_4 and 0.1 M KNO_3 solution.

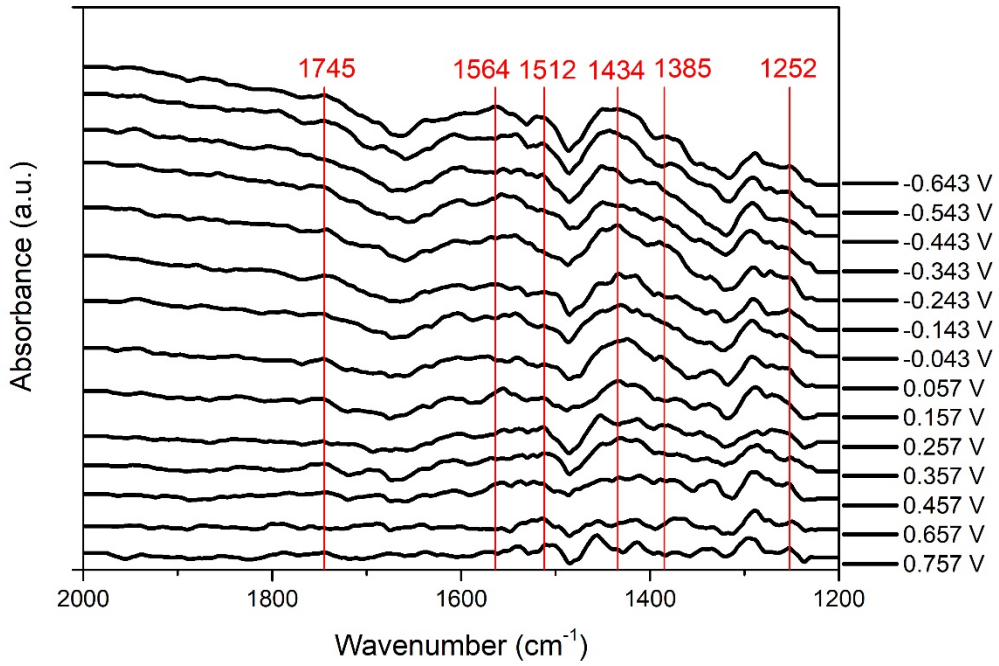

Figure S15. *In-situ* ATR-IR spectra of PdAg alloy working at different potential for NO_3RR.

Table S1. The electrochemical performances of Pd-based materials for NO_3RR.

Catalyst	Working potential (V vs RHE)	electrolyte	NO_3^- concentration	FE_{NH3} (%)	Yield rate	Ref.
PdAg alloy	-0.44	0.5 M K_2SO_4	0.1 M	97.47	0.683 mmol h^{-1} mg_{cat}^{-1} 11.609 mg h^{-1} mg_{cat}^{-1}	this work
Mesoporous PdN	-0.7	0.1 M Na_2SO_4	5.0×10^{-3} M	96.1	3760 μg h^{-1} mg^{-1}	1
PdBP NAs	-0.66	0.5M K_2SO_4	100 mg L^{-1}	64.73	0.109 mmol h^{-1} cm^{-2}	2
PdCu MC	-0.20	0.1 M KOH	10 mM	96.6	5.6 mg h^{-1} mg^{-1}	3
PdCu NPs/TiO_{2-x}	-1.4	0.5M Na_2SO_4	0.1 M	38.5	322.7 mmol h^{-1} cm^{-2}	4
$Pd_{74}Ru_{26}$ NC	-0.9	1 M KOH	100 mM	~100	42.98 mg h^{-1} cm^{-2}	5
ISAA In−Pd	-0.6	0.5M Na_2SO_4	100 mM	87.2	28.06 mg h^{-1} mg_{Pd}^{-1}	6
Cu/Pd/CuOx	-1.3	0.5 M K_2SO_4	50 mg L^{-1}	84.04	1510.3 μg h^{-1} mg_{cat}^{-1}	7
PdNi NS	-0.77	0.1 M $KHCO_3$	0.05 M	99.6	181 mmol h^{-1} cm^{-2}	8

1. *Adv. Mater.*, **2023**, *35*, 2207305.
2. *J. Mater. Chem. A*, **2022**, *10*, 16290.
3. *Adv. Mater.*, **2024**, *36*, 2402767.
4. *J. Mater. Chem. A*, **2023**, *11*, 22466.
5. *Chem. Sci.*, **2024**, *15*, 8204.
6. *J. Am. Chem. Soc.*, **2023**, *145*, 13957.
7. *Appl. Catal. B: Environ.*, **2022**, *318*, 121805.
8. *Chem. Commun.*, **2025**, *61*, 8544.